



Wind Field Simulation with Isogeometric Analysis

R. Montenegro*, J. M. Escobar*, J. López*, M. Brovka*,
A. Oliver*, G. Montero*, E. Rodríguez*, and G. V. Socorro-Marrero*

Abstract—

For wind field simulation with isogeometric analysis, firstly it is necessary to generate a spline parameterization of the computational domain, which is an air layer above the terrain surface. This parameterization is created with the mecano method from a digital terrain model. The main steps of the mecano method for tetrahedral mesh generation were introduced in [1, 2]. Based on the volume parameterization obtained by the method, we can generate a mapping from the parametric T-mesh to the physical space [3, 4]. Then, this volumetric parameterization is used to generate a cubic spline representation of the physical domain for the application of isogeometric analysis. We consider a mass-consistent model [5] to compute the wind field simulation in the three-dimensional domain from wind measurements or a wind forecasted by a meteorological model (for example, WRF or HARMONIE). From these data, an interpolated wind field is constructed. The mass-consistent model obtains a new wind field approaching the interpolated one, but verifying the continuity equation (mass conservation) for constant density and the impermeability condition on the terrain. This adjusting problem is solved by introducing a Lagrange multiplier, that is the solution of a Poisson problem. The resulting field is obtained from the interpolated one and the gradient of the Lagrange multiplier. It is well known that if we use classical Lagrange finite elements, the gradient of the numerical solution is discontinuous over the element boundary. The advantage of using isogeometric analysis with cubic polynomial basis functions [6, 7] is that we obtain a C^2 continuity for the Lagrange multiplier in the whole domain. In consequence, the resulting wind field is better approximated. Applications of the proposed technique are presented.

1 Introduction

One of the open problems of isogeometric analysis [8] is how to obtain a spline parameterization of the interior of a computational domain from the description of its boundary. CAD models usually provide only the boundary surface of a solid. The application of isogeometric analysis requires a full volumetric representation of the geometry. A parameterization is suitable for analysis if there are no self-intersections. Moreover, in order to obtain an accurate numerical result, it is necessary to have a good quality parameterization. Orthogonality and uniformity are desirable for the tensor-product structured parameterization. It is not a trivial task to obtain a good qual-

ity smooth global parametric mapping for complex domains, and it can be very time-consuming. IGA requires an effective method to construct a spline parameterization from the boundary of the object.

In this work, we propose a optimization-based approach. To obtain the parameterization of the object Ω (physical domain) we deform a T-mesh of the parametric domain, the unitary cube $\hat{\Omega} = [0, 1]^d$, $d = 2, 3$, until it achieves the shape of the object. This deformation only affects the positions of the nodes, that is, there is not any change in their connectivities: we say that both meshes are isomorphic. Given that a point can be fully determined by the local coordinates relative to the cell in which it is

*University Institute for Intelligent Systems and Numerical Applications in Engineering (SIANI), www.dca.iusiani.ulpgc.es/proyecto2015-2017, University of Las Palmas de Gran Canaria, Campus de Tafira, 35017 Las Palmas, Spain. Email: rafael.montenegro@ulpgc.es, josem.escobar@ulpgc.es, jilopez@siani.es, mbrovka@siani.es, albert.oliver@ulpgc.es, gustavo.montero@ulpgc.es, eduardo.rodriguez@ulpgc.es, gvsocorro.siani@upct.es

contained, we can define a one-to-one mapping between parametric domain $\widehat{\Omega}$ and the object. Mesh deformation is accomplished by means of the simultaneous T-mesh untangling and smoothing procedure based on a pointwise mean ratio quality measure. This quality metric gains both good orthogonality and uniformity of the isoparametric curves and forces the mapping to be as conformal as possible. Then, spline representation of the object is calculated by imposing interpolation conditions using the data provided by one-to-one correspondence between the mesh of the parametric domain and the mesh of the physical object. The interpolation is performed using polynomial spline spaces constructed via a technique proposed in our previous work [7]. This simple strategy allows to define easily a cubic spline space with nice properties over a given strongly balanced quadtree/octree T-mesh. However, any other spline basis defined over a T-mesh can be used.

The paper is organized as follows. In next section we describe the main steps of the proposed algorithm. Section 3 describes the T-mesh optimization procedure which is the key of the method. The modeling of the geometry by means of cubic splines is developed in Section 4. In Section 5 we show an example of the application of isogeometric analysis to wind simulation problem, where the domain is parameterized with our method. Finally, in section 6 we present the conclusions and set out some future lines.

2 General scheme of the method

The method is based on the ideas of our previous works on mesh untangling and smoothing and the Meccano method [9, 10, 11]. The algorithm includes the following stages:

1. *Construction of an adapted T-mesh:* An adapted T-mesh is generated by refining the initial mesh until the input boundary is approximated with a prescribed tolerance. During this process, the boundary nodes of the parametric domain are mapped to the boundary of the object.
2. *T-Mesh optimization:* The inner nodes of the physical T-mesh are relocated by applying a simultaneous untangling and smoothing procedure.
3. *Construction of a spline representation of the geometry:* Spline representation of the object is calculated by interpolating the data provided by the transformation between the parametric and physical meshes of the object.

The T-meshes used in this work are hierarchical meshes with a quadtree/octree structure, which are frequently used in engineering. Due to their simplicity, tree-structured meshes are an attractive tool for performing adaptive refinement in IGA and geometric modelling. For spline representation of the object we use polynomial spline spaces constructed via the technique described in [7]. This strategy allows to define easily a cubic

spline space with nice properties over a given strongly balanced quadtree/octree T-mesh.

3 T-mesh optimization

During construction of the adapted T-mesh in the step 1 of the method, the boundary $\widehat{\Gamma}_k$ of the adapted T-mesh $\widehat{\Omega}_k$ is mapped to the boundary of the object Γ , generating the surface Γ_k , which is the final approximation of Γ . The position of the inner nodes are determined by means of the T-mesh optimization procedure developed in this section, which is the key of the method. Once the inner nodes are relocated, the resulting physical T-mesh Ω_k is an approximation of the original geometry Ω . The corresponding piecewise volumetric parameterization is denoted as

$$(1) \quad \Pi : \widehat{\Omega}_K \rightarrow \Omega_K,$$

where any point p of a cell of $\widehat{\Omega}_K$ is mapped into a point q of the transformed cell of Ω_K by using an appropriate local mapping related to the cell.

To reduce the computational effort during the optimization process it is preferable to perform a previous relocation of the inner nodes. For this purpose Laplacian smoothing or Coons patch [12, 13] can be used. This previous relocation facilitates the untangling process, but in general does not obtain a satisfactory mesh quality and can produce self-intersections. Therefore, it is essential to apply an effective optimization algorithm. Figure 1(a) shows an example of the adapted parametric T-mesh constructed in the previous stage, Fig. 1(b) shows the tangled physical T-mesh after applying Coons patch, and Fig. 1(c) illustrates the resulting optimized T-mesh. An example of a 3D adapted parametric T-mesh and the corresponding optimized physical T-mesh of the solid is shown in Fig. 2.

The mesh optimization procedure consists in an iterative process where each node is moved to a new position in order to improve the quality of the *local submesh*, which is the set of elements connected to the free node. This new position of the node is determined by minimizing an objective function based on the *mean ratio* shape quality measure. This algebraic quality measure was originally introduced for a triangle, and it is defined in terms of the Jacobian matrix of the affine mapping from the ideal (target) triangle to the given one. It represents the deviation of the given triangle from the ideal one. The distortion of an element is defined as the inverse of its quality.

The objective function for a given free node is constructed as a sum of shape distortion measures of all elements of its local submesh. For each cell of the physical T-mesh, the corresponding parametric cell is used as its ideal element. Repeating the optimization procedure for all inner nodes we achieve to minimize the deformation of the physical mesh with respect to the parametric one.

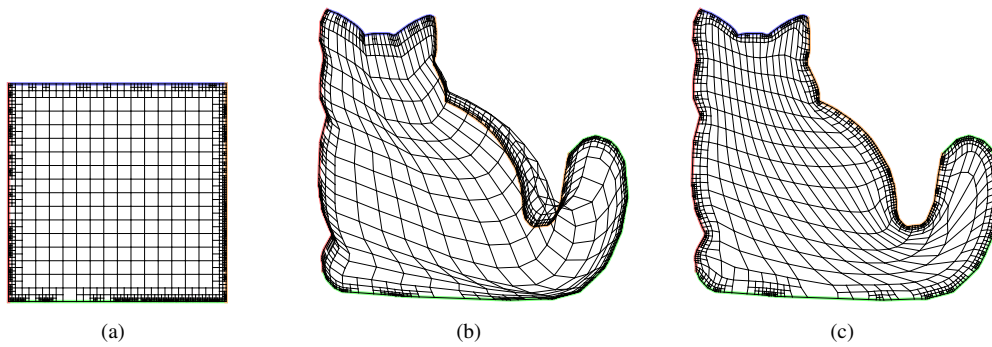


Figure 1: Stages of T-mesh construction for the *Cat* test model geometry. (a) Parametric T-mesh adapted to the boundary of the geometry; (b) previous relocation by Coons patch, tangled mesh; (c) optimized physical T-mesh. The color lines represent the correspondence between the parametric and physical boundaries.

3.1 Jacobian-based shape quality measure for a triangle/tetrahedral mesh optimization

Here we briefly revise the concept of algebraic shape quality metric for a linear simplex element, see [14, 15], and the objective function we use for a linear triangle/tetrahedral mesh optimization. For more details see [1, 11, 16, 3].

Let S be the Jacobian matrix of the affine mapping that takes the ideal element (target) τ_I into the physical d -simplex element τ ($d = 2, 3$). Then, quality metrics of the simplex τ can be defined in terms of the matrix S . For example, *mean ratio*

$$q = \frac{d \sigma^{2/d}}{\|S\|^2},$$

is a scale, rotation and translation invariant algebraic quality metric of τ , where $\sigma = \det(S)$ and $\|S\|$ is the Frobenius norm of S . The maximum value of q is 1, and it is reached when $S = \mu R$, where μ is a scalar and R is a rotation matrix. In other words, q attains its maximum if and only if τ and τ_I are similar (same shape). Besides, any degenerate simplex has quality measure 0. The distortion measure is defined as the inverse of its quality, i.e.,

$$\eta = \frac{1}{q} = \frac{\|S\|^2}{d \sigma^{2/d}}.$$

Let $\mathbf{x} \in \mathbb{R}^d$ be a free node whose new position is to be determined. The objective function to be minimized is defined as

$$K(\mathbf{x}) = \frac{1}{N} \sum_{i=1}^N \eta_i = \frac{1}{N} \sum_{i=1}^N \frac{\|S_i\|^2}{d \sigma_i^{2/d}},$$

where N is the number of elements connected to the free node \mathbf{x} and η_i is the distortion measure for the i -th element of the local mesh.

The objective function K becomes discontinuous when the area of any triangle tends to zero. Due to these singularities, the

function K improves the quality of valid elements but it does not work properly when the mesh is tangled ($\sigma \leq 0$). In [11] we proposed a modification of K by replacing the determinant σ by the positive, smooth and increasing function $h(\sigma) = \frac{1}{2}(\sigma + \sqrt{\sigma^2 + 4\delta^2})$. Then, the modified distortion becomes

$$\eta^* = \frac{\|S\|^2}{d h(\sigma)^{2/d}}.$$

This modification eliminates the asymptotes associated with their singularities and the new objective function

$$K^*(\mathbf{x}) = \frac{1}{N} \sum_{i=1}^N \eta_i^*$$

becomes smooth in \mathbb{R}^d . In the feasible region (subset of \mathbb{R}^d where the free node could be placed for the local mesh to be valid) the modified objective function K^* approximates the original function K as $\delta \rightarrow 0$, and then, the minimum of the original and modified objective functions are nearly identical when δ is small. When this region does not exist, the minimum of the modified objective function is located in such a way that it tends to untangle the local mesh. Thus, the modified objective function allows the simultaneous untangling and smoothing of the mesh. The value of δ is selected in terms of the local mesh under consideration, making it as small as possible and in such a way that the evaluation of the minimum of the modified function does not present any computational problem. For more details see [11, 17]. The unconstrained optimization problem can be easily solved with any standard method.

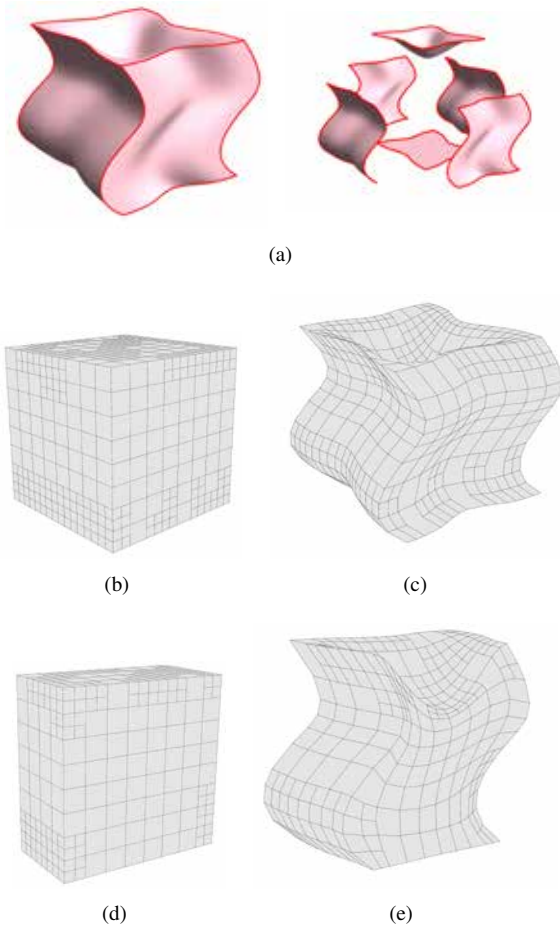


Figure 2: Test model 1. (a) Parametric T-mesh adapted to the boundary of the geometry; (b) optimized physical T-mesh; (c) a section of parametric T-mesh; (d) a section of physical T-mesh.

3.2 Jacobian-based shape quality metric for arbitrary elements

To extend the concept of the shape quality metric for non-simplicial elements (or for a higher-order simplicial ones) with non-constant Jacobian matrix we introduce the following concepts.

Let Ω_e be any type physical cell of the local mesh for the free node \mathbf{x} . First, we define a pointwise distortion measure for the given cell using some appropriate mapping $\mathbf{G} : \widehat{\Omega}_e \rightarrow \Omega_e$ from the ideal element to the physical one. Here, we use quadratic isoparametric mapping.

Let $J_G(\xi)$ be the Jacobian matrix of the mapping \mathbf{G} at point ξ . Then, the modified distortion at any point ξ of the ideal element is defined as

$$\eta^*(\xi) = \frac{\|J_G(\xi)\|^2}{dh(\sigma(\xi))^{2/d}}, \quad \xi \in \widehat{\Omega}_e.$$

where $\sigma(\xi) = \det(J_G(\xi))$.

To assess the distortion of the entire physical element Ω_e we can define a global distortion measure by means of L^1 norm of the pointwise distortion, namely

$$(2) \quad \eta_{\Omega_e}^* = \frac{1}{V_{\widehat{\Omega}_e}} \int_{\widehat{\Omega}_e} \eta^*(\xi) d\widehat{\Omega}_e,$$

where $V_{\widehat{\Omega}_e}$ is the volume of $\widehat{\Omega}_e$. Other norms, for example L^2 , can be used.

The global modified distortion $\eta_{\Omega_e}^*$ takes values between 1 and ∞ . If the physical element Ω_e coincides with the ideal one, then $\eta^*(\xi) \rightarrow 1$ when $\delta \rightarrow 0$. On the other hand, this global distortion measure presents *pseudo-barriers*, that is, $\eta_{\Omega_e}^* \rightarrow \infty$ when $\sigma(\xi) \leq 0$ and $\delta \rightarrow 0$.

The global quality of the element is defined as the inverse of its global distortion, i.e.

$$q_{\Omega_e}^* = \frac{1}{\eta_{\Omega_e}^*},$$

and it takes values from $[0, 1]$.

We define the objective function for a free node \mathbf{x} using the introduced global distortion measure for the cells

$$(3) \quad K^*(\mathbf{x}) = \frac{1}{N} \sum_{i=1}^N \eta_{\Omega_i}^*(\mathbf{x}),$$

being N the number of cells connected to the free node \mathbf{x} and $\eta_{\Omega_i}^*(\mathbf{x})$ the global distortion measure for the i -th cell.

The integral is evaluated by a numerical quadrature. Let $\{\xi_j\}_{j=1,M}$ be a set of quadrature points over the ideal element $\widehat{\Omega}_e$. Then the objective function for the free node \mathbf{x} becomes

$$(4) \quad K^*(\mathbf{x}) = \frac{1}{N} \sum_{i=1}^N \left(\sum_{j=1}^M w_j \eta_{\Omega_i}^*(\xi_j) \right),$$

where w_j is the corresponding weight for the quadrature point ξ_j . Thus, in practice, the objective function is based on the pointwise distortion measure, evaluated at certain set of sample points within the ideal cell. Analogously to the triangular mesh, the unconstrained optimization problem can be easily solved with any standard method. To maintain a low computational cost of the minimization, it is preferable to use a few quadrature points. Also, it is preferable to evaluate the quality at the corner vertices of the cell, because usually the major distortion occurs at these points. Therefore, we use Gauss-Lobatto quadrature rule that includes boundary quadrature points. More specifically, we use three quadrature points $\{-1, 0, 1\}$ of the reference interval $[-1, 1]$.

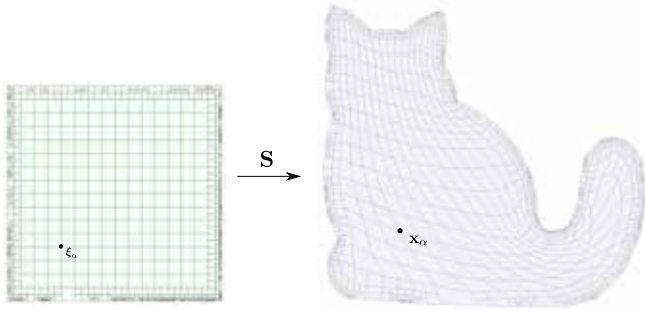


Figure 3: *Cat* test model. Parametric domain and spline representation of the physical domain.

4 Construction of a spline representation of the geometry

In this section we construct a spline representation of the geometry. For simplicity, the process is described for 2D, being the generalization to 3D obvious.

We have to obtain a global one-to-one spline transformation $\mathbf{S} : \hat{\Omega} = [0, 1]^2 \rightarrow \Omega$ that maps the parametric domain into the physical one. For this purpose, we use polynomial spline spaces constructed via the strategy proposed in our previous work [7, 6]. This strategy allows to define easily cubic spline spaces with nice properties over a given strongly balanced quadtree/octree T-mesh. We are going to refer to these spline functions as Extended Polynomial splines (EP-splines). According to the strategy, each regular node of the T-mesh has one blending function assigned. Similarly to T-splines [18], local knot vectors for each function are inferred by walking across the mesh and traversing its edges. Then, in order to span spaces with nice properties, some of the inferred function supports have to be modified applying certain modification rules.

4.1 Interpolation

Spline representation of the physical domain is build as a linear combination of EP-spline blending functions defined over the adapted parametric T-mesh T

$$\mathbf{S}(\xi) = \sum_{\alpha \in A_T} \mathbf{P}_\alpha \hat{N}_\alpha(\xi),$$

where $\mathbf{P}_\alpha \in \mathbb{R}^2$ is the control point corresponding to the α -th blending function.

Control points \mathbf{P}_α are found by imposing interpolation conditions. A standard choice for an interpolation with B-splines is Greville abscissae, which is the averages of the knots. These points correspond approximately to the points where the B-spline functions attain their maximum. The generalization of this concept for the T-mesh leads to the so-called Greville collocation points. Dealing with a T-mesh, we do not have a global

knot vector, so a set of Greville points is obtained as the knot average of each local knot vector, that is, for the local knot vectors $\Xi_\alpha = \{\xi_1, \xi_2, \xi_3, \xi_4, \xi_5\}$ and $\mathcal{H}_\alpha = \{\eta_1, \eta_2, \eta_3, \eta_4, \eta_5\}$ of the function N_α , its Greville point is defined as $\xi_\alpha = (\xi_\alpha, \eta_\alpha)$, where

$$\xi_\alpha = \frac{\xi_2 + \xi_3 + \xi_4}{3} \quad \text{and} \quad \eta_\alpha = \frac{\eta_2 + \eta_3 + \eta_4}{3}.$$

In the case of our EP-spline functions, Greville points coincide with their anchors and thus with the vertices of the T-mesh, except for the functions that contain three repeated boundary knots. For each point ξ_β in the parametric space its image \mathbf{x}_β in the physical space is determined by the piece-wise mapping Π obtained by the mesh optimization process developed in section 3.

Finally, the control points are found from the linear system of equations

$$\mathbf{x}_\beta = \mathbf{S}(\xi_\beta) = \Pi(\xi_\beta) = \sum_{\alpha \in A_T} \mathbf{P}_\alpha \hat{N}_\alpha(\xi_\beta), \quad \forall \xi_\beta, \beta \in A_T.$$

We remark that the construction of the spline representation can also be performed with any other spline basis functions defined over a T-mesh.

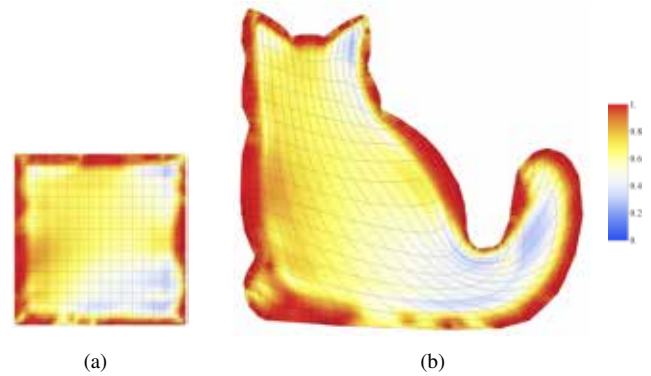


Figure 4: *Cat* test model. Colormap of mean ratio Jacobian. (a) Parametric domain. (b) Physical domain.

4.2 Quality assessment of the mapping. Mean ratio Jacobian

To assess the pointwise quality of the obtained parameterization we appeal to the same idea used in the optimization procedure. Namely, our objective function was based on the pointwise quality measure of the local quadratic mapping for each cell. Now we can analyze the pointwise quality measure of the constructed spline transformation. That is, we calculate at each point of the domain the mean ratio Jacobian given by

$$q_S(\xi) = \frac{d \det(J_S)^{2/d}}{\|J_S\|^2},$$

where J_S is the Jacobian matrix of the mapping \mathbf{S} at the point ξ of the parametric domain. In contrast to the scaled Jacobian, that represents the quality of the mapping \mathbf{S} in the sense of the orthogonality of its isoparametric curves, the mean ratio Jacobian represents both: a quality in the sense of the orthogonality and uniformity. The mean ratio Jacobian equals 1 at the point \mathbf{P}_0 if the mapping conserves orthogonality and produces the same length distortion in both parametric directions, i.e. the mapping is conformal at this point.

Figure 4 shows the resulting spline representation of the *Cat* test model and the colormap of the mean ratio Jacobian, whose minimal value is 0.26.

Figure 5 shows 3D parameterization example with its corresponding colormap of mean ratio Jacobian, whose minimal value is 0.34.

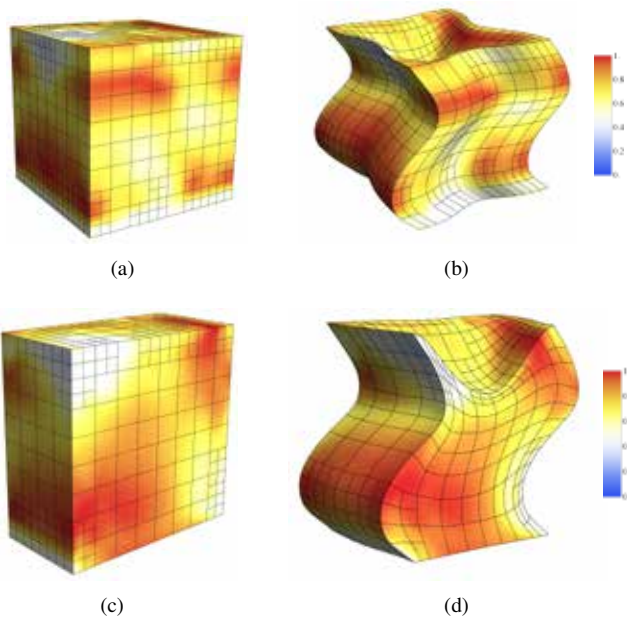


Figure 5: Test model 1. Colormap of mean ratio Jacobian. (a) Parametric domain; (b) spline representation of the physical domain; (c) a section of the parametric domain; (d) corresponding section in the physical domain.

5 Isogeometric analysis applications. Wind field adjustment problem

The problem of wind field adjustment consists in finding a velocity field \vec{u} over a certain complex terrain that offers the best adjustment to some initial field \vec{u}_0 obtained from experimental measures. We use a mass consistent model based on the continuity equation of an incompressible flow with an imper-

meability boundary condition on the terrain surface Γ_b

$$(5) \quad \nabla \cdot \vec{u} = 0 \quad \text{in } \Omega$$

$$(6) \quad \vec{n} \cdot \vec{u} = 0 \quad \text{on } \Gamma_b$$

To find a field $\vec{u} = (u, v, w)$, adjusted to the given initial field $\vec{u}_0 = (u_0, v_0, w_0)$, we formulate a least-square problem in the domain Ω with the functional for a field $\vec{v} = (\tilde{u}, \tilde{v}, \tilde{w})$

$$(7) \quad E(\vec{v}) = \int_{\Omega} [(\tilde{u} - u_0)^2 + (\tilde{v} - v_0)^2 + (\tilde{w} - w_0)^2] d\Omega.$$

Then the velocities field \vec{u} is the solution of the following problem: Find $\vec{u} \in \mathbb{K}$ such that

$$(8) \quad E(\vec{u}) = \min_{\vec{v} \in \mathbb{K}} E(\vec{v})$$

$$\mathbb{K} = \{\vec{v} : \nabla \cdot \vec{v} = 0, \vec{n} \cdot \vec{v} = 0 \text{ on } \Gamma_b\}.$$

This problem is equivalent to find a saddle point (\vec{u}, λ) of the Lagrangian

$$(9) \quad L(\vec{v}, \lambda) = E(\vec{v}) + \int_{\Omega} \lambda \nabla \cdot \vec{v} d\Omega,$$

being $\lambda(x, y, z)$ the Lagrange multiplier.

Then the resulting wind field \vec{u} verifies the Euler-Lagrange equations

$$(10) \quad \vec{u} = \vec{u}_0 + \nabla \lambda.$$

Substituting (10) into (5) and (6), the variational approach results in an elliptic problem for λ

$$(11) \quad \begin{aligned} -\Delta \lambda &= \nabla \cdot \vec{u}_0 \quad \text{in } \Omega \\ -\vec{n} \cdot (\nabla \lambda) &= \vec{n} \cdot \vec{u}_0 \quad \text{on } \Gamma_b \\ \lambda &= 0 \quad \text{on } \Gamma_a \end{aligned}$$

For more details about wind field adjustment model see [19, 20].

Numerical solution for the function λ is found via isogeometric analysis. Then, we obtain the wind field \vec{u} from equation (10). Here we solve the problem over the orography of the *La Palma* island with a constant initial wind velocity $\vec{u}_0 = (10, 0, 0)$ m/s. To solve the elliptic problem (11) we need to construct a domain parameterization adapted to the singularities of the terrain. Figure 6(a) shows the interior of the computational domain, which includes a 10 km air layer above the terrain surface. Streamlines of the adjusted wind field \vec{u} are shown in Fig. 6(b). The black arrow indicates the direction of the initial wind velocity \vec{u}_0 . It can be observed that the red streamlines started from the points close to the surface tend to follow the terrain orography. The blue streamlines start at the points with the same x, y coordinates but higher z coordinate, and it can be appreciated that they are less influenced by the orography.

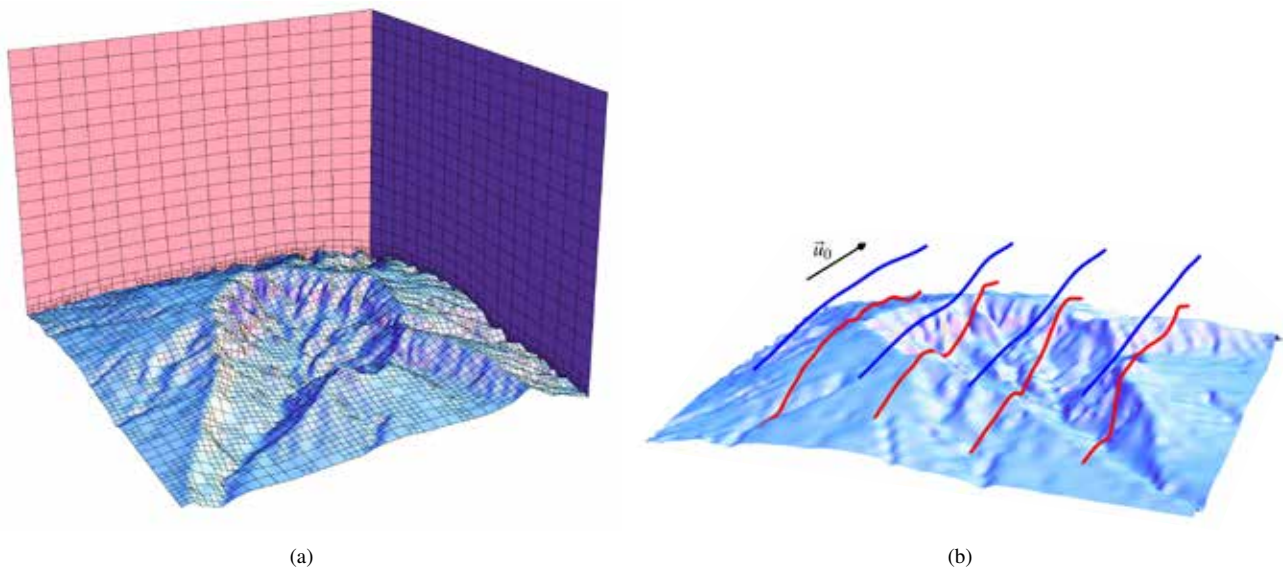


Figure 6: Wind field adjustment problem. (a) The interior of the computational domain (a 10 km air layer above the terrain surface). (b) Streamlines of the adjusted field \vec{u} . Red streamlines start from the points situated 300 m above terrain surface; blue streamlines start from the points with the same x, y coordinates and at height of 1500 m.

6 Conclusions and challenges

We have presented an affective tool for obtaining a single patch spline parameterization for 2D and 3D geometries. A new T-mesh untangling and smoothing procedure has been applied in order to define an isomorphic transformation between parametric and physical T-meshes. This transformation provides the data to perform interpolation and construct a spline representation of the object. The presented technique is simple and easy to implement. The algorithm has been tested in several 2D and 3D geometries and, for all of them, we have obtained a high quality parametric transformation with strictly positive Jacobian. Also, we have presented an example of application of isogeometric analysis to wind field simulation problem, where the domain is parameterized with our technique. In our future work we plan to develop a more direct parameterization approach based on optimization of the control points of the spline mapping instead of its piecewise approximation.

Acknowledgements

Supported by FEDER and the Spanish Government, "Ministerio de Economía y Competitividad", grant contract: CTM2014-55014-C3-1-R; and by CONACYT-SENER, grant contract: 163723.

References

- [1] R. Montenegro, J. M. Cascón, J. M. Escobar, E. Rodríguez, G. Montero, An automatic strategy for adaptive tetrahedral mesh generation, *Appl. Num. Math.* 59 (2009) 2203–2217.
- [2] J. M. Cascón, E. Rodríguez, J. M. Escobar, R. Montenegro, Comparison of the meccano method with standard mesh generation techniques, *Engineering with Computers* 31 (1) (2015) 161–174.
- [3] J. M. Escobar, J. M. Cascón, E. Rodríguez, R. Montenegro, A new approach to solid modeling with trivariate T-splines based on mesh optimization, *Comput. Meth. Appl. Mech. Eng.* 200 (2011) 3210–3222.
- [4] J. M. Escobar, J. M. Cascón, E. Rodríguez, R. Montenegro, The meccano method for isogeometric solid modeling, in: *Proc. of the 20th International Meshing Roundtable*, Springer, Berlin, 2011, pp. 551–568.
- [5] A. Oliver, E. Rodríguez, J. M. Escobar, G. Montero, M. Hortal, J. Calvo, J. M. Cascón, R. Montenegro, Wind forecasting based on the harmonie model and adaptive finite elements, *Pure and Applied Geophysics* 172 (1) (2015) 109–120.
- [6] M. Brovka, Construction of polynomial spline spaces over T-meshes for its application in Isogeometric Analysis, Ph.D. thesis, Universidad de Las Palmas de Gran Canaria.
- [7] M. Brovka, J. I. López, J. M. Escobar, R. Montenegro, J. M. Cascón, A simple strategy for defining polynomial spline spaces over hierarchical T-meshes, *Computer-Aided Design* 72 (2016) 140–156.

- [8] Y. Bazilevs, V. M. Calo, J. A. Cottrell, J. A. Evans, T. J. R. Hughes, S. Lipton, M. A. Scott, T. W. Sederberg, Isogeometric analysis: Toward unification of computer aided design and finite element analysis, in: Trends in Engineering Computational Technology, Saxe-Coburg Publications, Stirling, 2008, pp. 1–16.
- [9] J. M. Cascón, R. Montenegro, J. M. Escobar, E. Rodríguez, G. Montero, A new *meccano* technique for adaptive 3-D triangulation, in: Proc. of the 16th International Meshing Roundtable, Springer, Berlin, 2007, pp. 103–120.
- [10] J. M. Cascón, R. Montenegro, J. M. Escobar, E. Rodríguez, G. Montero, The *meccano* method for automatic tetrahedral mesh generation of complex genus-zero solids, in: Proc. of the 18th International Meshing Roundtable, Springer, Berlin, 2009, pp. 463–480.
- [11] J. M. Escobar, E. Rodríguez, R. Montenegro, G. Montero, J. M. González-Yuste, Simultaneous untangling and smoothing of tetrahedral meshes, *Comput. Meth. Appl. Mech. Eng.* 192 (2003) 2775–2787.
- [12] S. A. Coons, *Surfaces for computer aided design*, Springfield, 1964.
- [13] G. Farin, D. Hansford, Discrete Coons patches, *Comput. Aid. Geom. Design* 16 (1999) 691–700.
- [14] P. M. Knupp, Algebraic mesh quality metrics, *SIAM J. Sci. Comput.* 23 (2001) 193–218.
- [15] P. M. Knupp, A method for hexahedral mesh shape optimization, *Int. J. Num. Meth. Eng.* 58 (2) (2003) 319–332.
- [16] J. M. Escobar, R. Montenegro, E. Rodríguez, J. M. Cascón, The *meccano* method for isogeometric solid modeling and applications, *Engineering with Computers* 30 (3) (2014) 331–343.
- [17] J. M. Escobar, E. Rodríguez, R. Montenegro, G. Montero, J. M. González-Yuste, SUS Code: Simultaneous mesh untangling and smoothing code, *Technote*, <http://www.dca.iusiani.ulpgc.es/SUScode/TechNote.pdf> (2003).
- [18] T. W. Sederberg, J. Zheng, A. Bakenov, A. Nasri, T-splines and T-NURCCs, *ACM Trans. Graph.* 22 (2003) 477–484.
- [19] G. Montero, R. Montenegro, J. Escobar, A 3-d diagnostic model for wind field adjustment, *Journal of Wind Engineering and Industrial Aerodynamics* 74-76 (1998) 249 – 261.
- [20] L. Ferragut, R. Montenegro, G. Montero, E. Rodriguez, M. Asensio, J. Escobar, Comparison between 2.5-d and 3-d realistic models for wind field adjustment, *Journal of Wind Engineering and Industrial Aerodynamics* 98 (2010) 548 – 558.